Non-linear analysis of seismic regime response to electromagnetic powerful source actions.

O. Yu. Melchaeva, S.B. Turuntaev
IDG RAS, Moscow

Abstract

A possibility to change seismic regime characteristics by strong electromagnetic field excitation in rocks was previously studied by several researches. The experimental research works, which were conducted at Garm, Tadzhikistan, and Bishkek, Kyrgyzstan, test sites showed short-time increase in the daily number of minor earthquakes, a concentration of the earthquake epicenters near the electromagnetic field source and some others aftereffects of the EM-field excitation. Meanwhile both physical mechanism of EM action on seismic processes and confident detection of EM seismic effects as well as their spatial-temporal limits are not resolved yet definitely.

In the presented report a study of strong EM pulse actions on seismic regime in the region of Bishkek test site is made with the help of non-linear dynamics methods.

Data characteristics.

As a source of EM actions, a powerful electroprospecting installation ERGU-600-2 was used. Probing pulse of ERGU-600-2 represents a series of periodic sign-changing square pulses of a current with amplitudes 600-800A and the period 10 sec. Duration of one session was about 20 minutes. The analysis of seismic activity was made on the basis of local seismic network data (KNET, Fig.1). The catalog contains 6623 earthquakes with magnitudes M=1-6, registered from 6.01.1994 till 12.30.2008 on the area with coordinates φ =37.35-45.77 N; λ =68.67-82.24 E.

The considered area of possible EM excitation influence was 200x200 km in size with center coincident with EM source position.

Analysis methods.

The study of the seismic activity variations were made by means of phase portrait reconstructions and calculations of the portrait parameters (an embedding space dimensionality and correlation dimension of an attractor, if that one exists). The earthquake catalog was divided into two parts of the same durations: before EM excitations and during the excitations. Seismic activity was calculated as sum of cubic roots from energies of seismic events occurred during a week (3 days overlap of the time intervals was used). The obtained time series were analyzed with the help of Grassberger-Procaccia method of correlation integral calculation for different embedding space dimensions. The integral was calculated as follows:

$$C(\varepsilon) = \frac{1}{N^2}\sum_{\substack{i,j=1\\ i\neq j}}^{N} \theta\left(\varepsilon - \left\| z_i - z_j \right\|\right)$$

where $\vec{z}_i$ is the vector describing position of a point in phase space at the moment of time $t_i = t_0 + i\tau, i = 1...N$

τ is the time delay, *N* is the sample volume, $\theta(x)$ is the Heaviside's function:

$$\theta(x) = \begin{cases} 1, x \geq 0; \\ 0, x < 0. \end{cases}$$

The value $C(\varepsilon)$ defines relative number of pairs points the distance between which is no more than ε. At small d the correlation integral

$$C(\varepsilon) \propto \varepsilon^d$$

therefore attractor's dimension *d* can be estimated on an inclination of dependence $\ln C$ from $\ln \varepsilon$:

$$\log C(\varepsilon) \cong d \log \varepsilon + c$$

Parameters of time delay were chosen based on autocorrelation functions.

Results

Change of the seismic activity in time is shown in Fig. 2 and Fig.3 for the time periods before EM action start and during actions of EM source, respectively.

The correlation integral was calculated for several embedded space dimensions, which were varied from 1 to 20. Time delay values were chosen based on autocorrelation function (Fig.4); their meanings are shown in Fig.5. Obtained relations between fractal correlation dimensionality and dimensions of embedded phase space are shown in Fig.5. It can be concluded that after start of EM actions the correlation dimensionality diminishes from 7.4-7.8 to 4.7-5.2, the embedded space dimensionality decreases from 14 to 6.

It can be supposed that some natural perturbations of seismic regime (an increase of seismic activity) could influence on the above results. To avoid it, calculations were made for the periods of observations, which have no significant peculiarities. The periods are shown in Fig.2 and Fig.3 by rectangular. Dependences of the correlation dimensionality on embedded space dimensions are shown in Fig.6. It can be seen, that before the EM action start, the seismic process didn't show any stable state indications, while during EM action the seismic process gains an attractor of dimensionality 5.6-6.0.

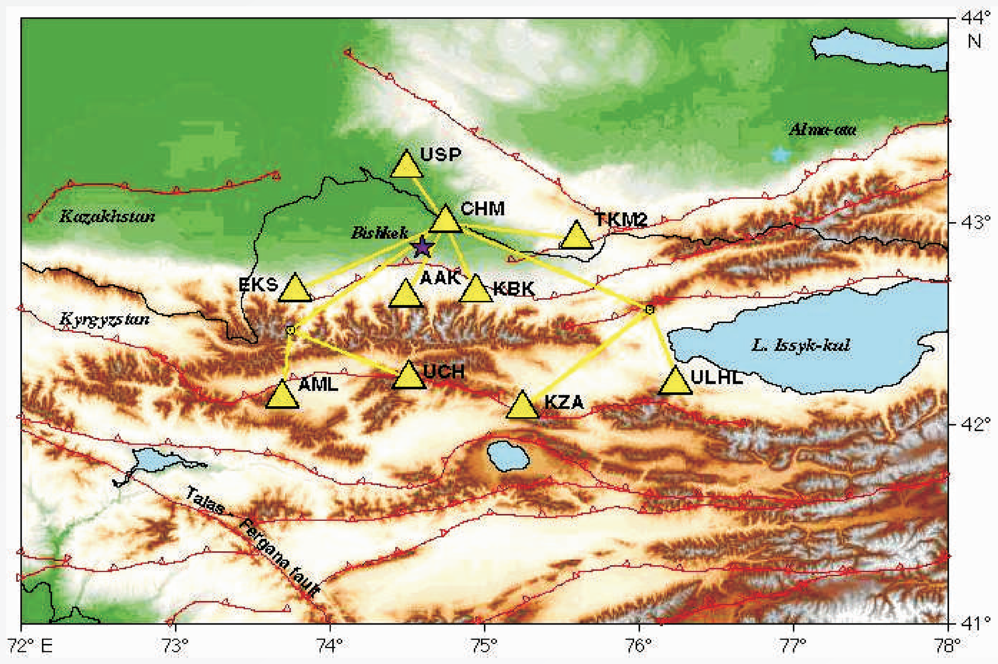

Fig. 1. Map of the studied region and KNET seismic station locations. Telemetry links are shown by yellow lines.

A	B_1	B_2	L_1	L_2	v*
$5*10^4$Pa	$1*10^5$Pa	$1*10^4$Pa	$1*10^{-2}$m	$1*10^{-3}$m	10^{-1}ms^{-1}

Table 1. Parameters of "rate-and-state" equation.

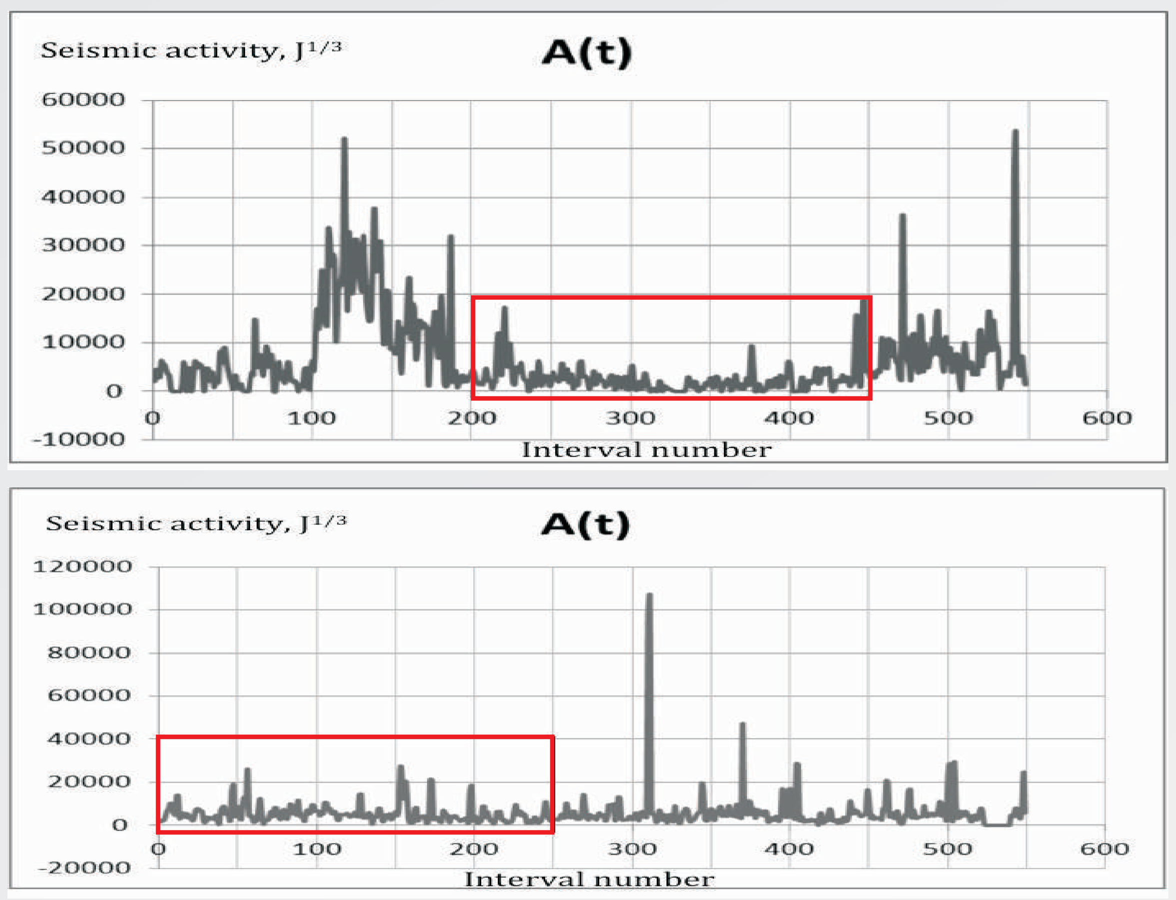

Fig.3. Change of the seismic activity in time during EM actions.

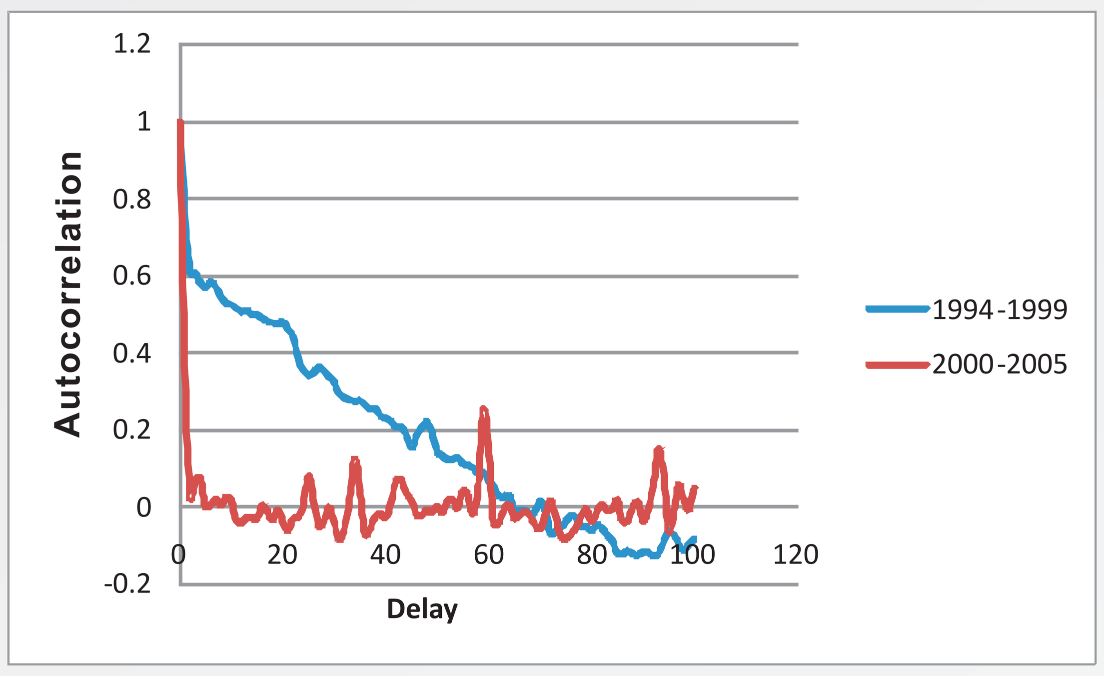

Fig.4. Autocorrelation function before and during EM actions.

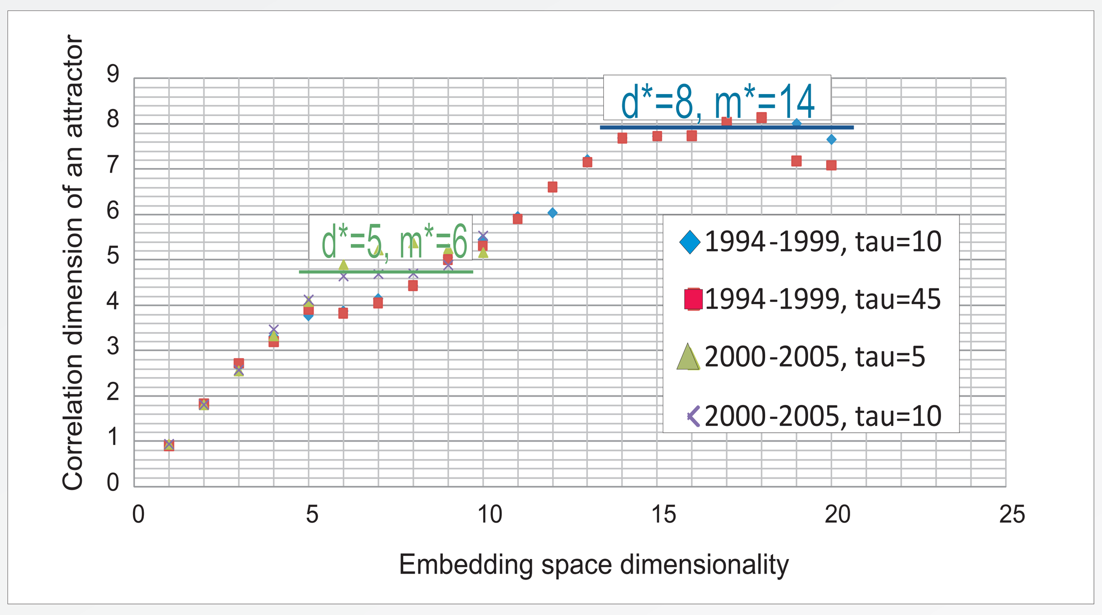

Fig.5. Fractal correlation dimension vs. embedding space dimensionality of the seismic activity before and during EM actions.

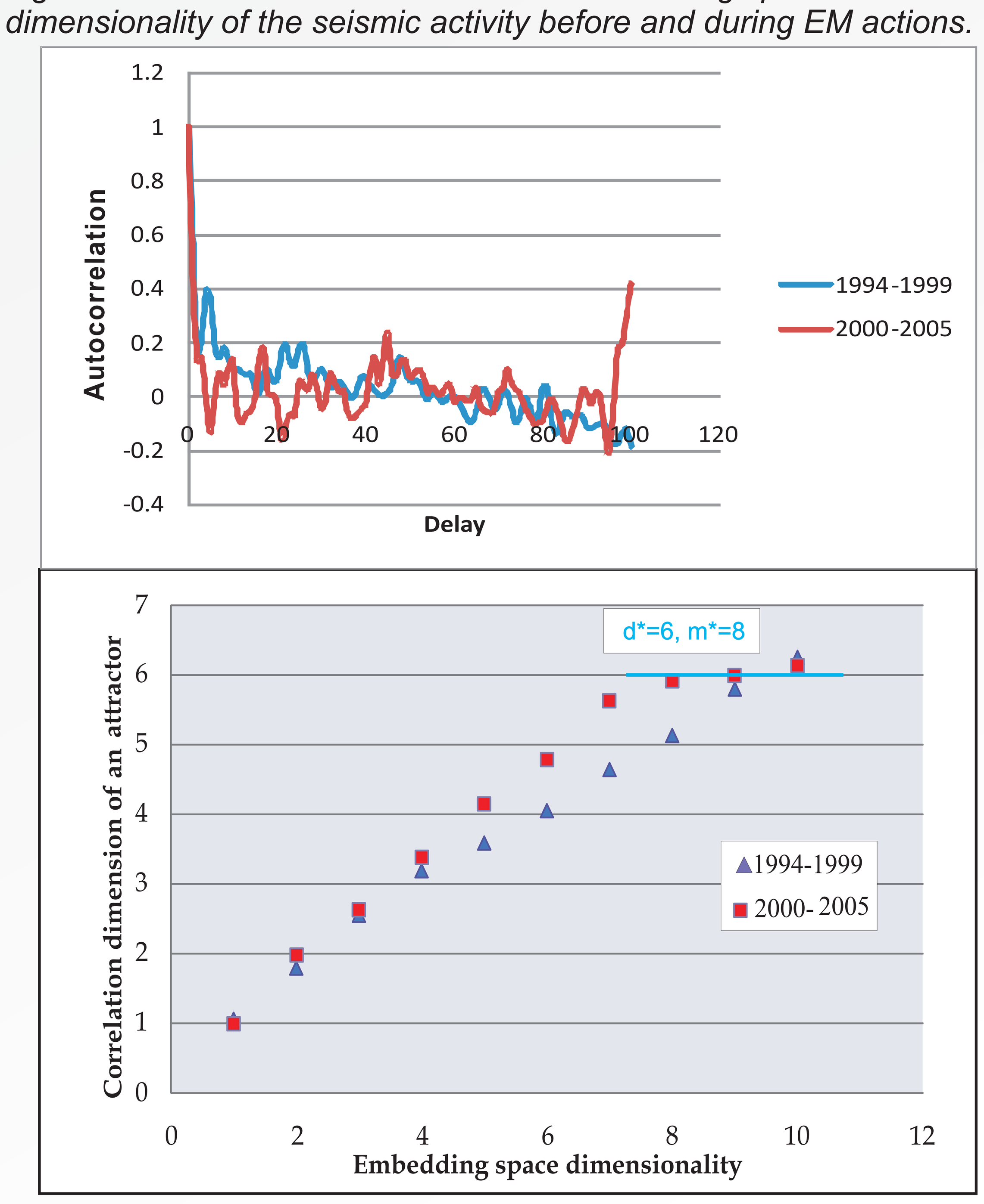

Fig.6. Autocorrelation functions (up graph) and fractal correlation dimension vs. embedding space dimensionality of the seismic activity before and during EM actions for time periods without peculiarities..

Model

To analyze the obtained results, we consider the widely used "stick-clip" model of seismic regime with "rate-and-state' friction law for description of the movements along tectonic faults. The main distinctions of used approach from the common one are the followings: we consider two-parameters type of the friction law and we vary the value of critical shear stress. The motion equation can be written as $m\ddot{u} = k(\upsilon t - u) - \tau s$

where *k* is stiffness, *v* is velocity at infinity, τ is frictional shear stress, which can be written as

$$\tau = \tau^* + A\ln(\upsilon/\upsilon^*) + \theta_1 + \theta_2$$

Here τ* is critical shear stress, which can be changed by EM actions,

$$\tau^* = C + \mu(\sigma - p)$$

C – cohesion, μ – friction coefficient, p – pore pressure, σ – normal stress, θ - state variable which characterizes sliding surface state:

$$\dot{\theta}_i = -\frac{\upsilon}{L_i}\left(\theta_i + B_i \ln\left(\frac{\upsilon}{\upsilon^*}\right)\right)$$

where L_i are characteristic dimensions of the fault roughness. Values of parameters in the above equations were taken from experiments Gu et al., 1984, and are shown in Table 1.

Results of numerical calculations for several values of critical stresses are shown in Fig.7 as projections of phase trajectories on τ-*v* plane. Dependencies of shear stresses on time and displacement on time are shown in Fig.8. The time is in arbitrary units.

It was found that if the critical stresses increase, system behavior changes significantly. Oscillations of the fault sliding become nonharmonic, and when the critical stresses reach 45 MPa, the oscillations become quasi-chaotic (Fig.8). An estimation of the obtained attractor dimensions by Grassberge-Procaccia method showed, that an increase of critical stresses results in increase of attractor correlation dimensionality: τ*=5MPa – 1.4; τ*=15MPa – 1.8; τ*=45MPa – >3.

Conclusions

The obtained results show an increase of seismic regime regularity after beginning of powerful EM pulses action: before EM excitation, the correlation dimensionality of the possible attractor was not less than 8 with corresponding embedded space dimension 14. After start of EM excitations, the attractor correlation dimensionality diminished to 4.6, embedded space dimension – to 6.

The model of possible reaction of the geomechanical system governed by rate-and-state friction law on perturbations due to EM actions is considered numerically. It was found, that change of fault and fracture strengths under EM action leads to diminishing of attractor and embedded space dimensions.

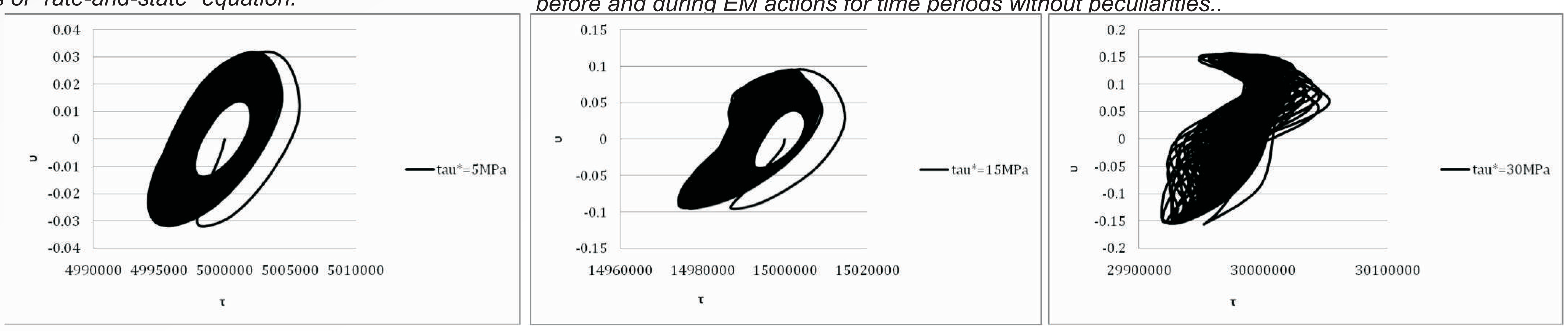

Fig.7.Projections of phase trajectories of a fault sliding on τ-*v* plane (shear stress - velocity) for several values of critical shear stresses.

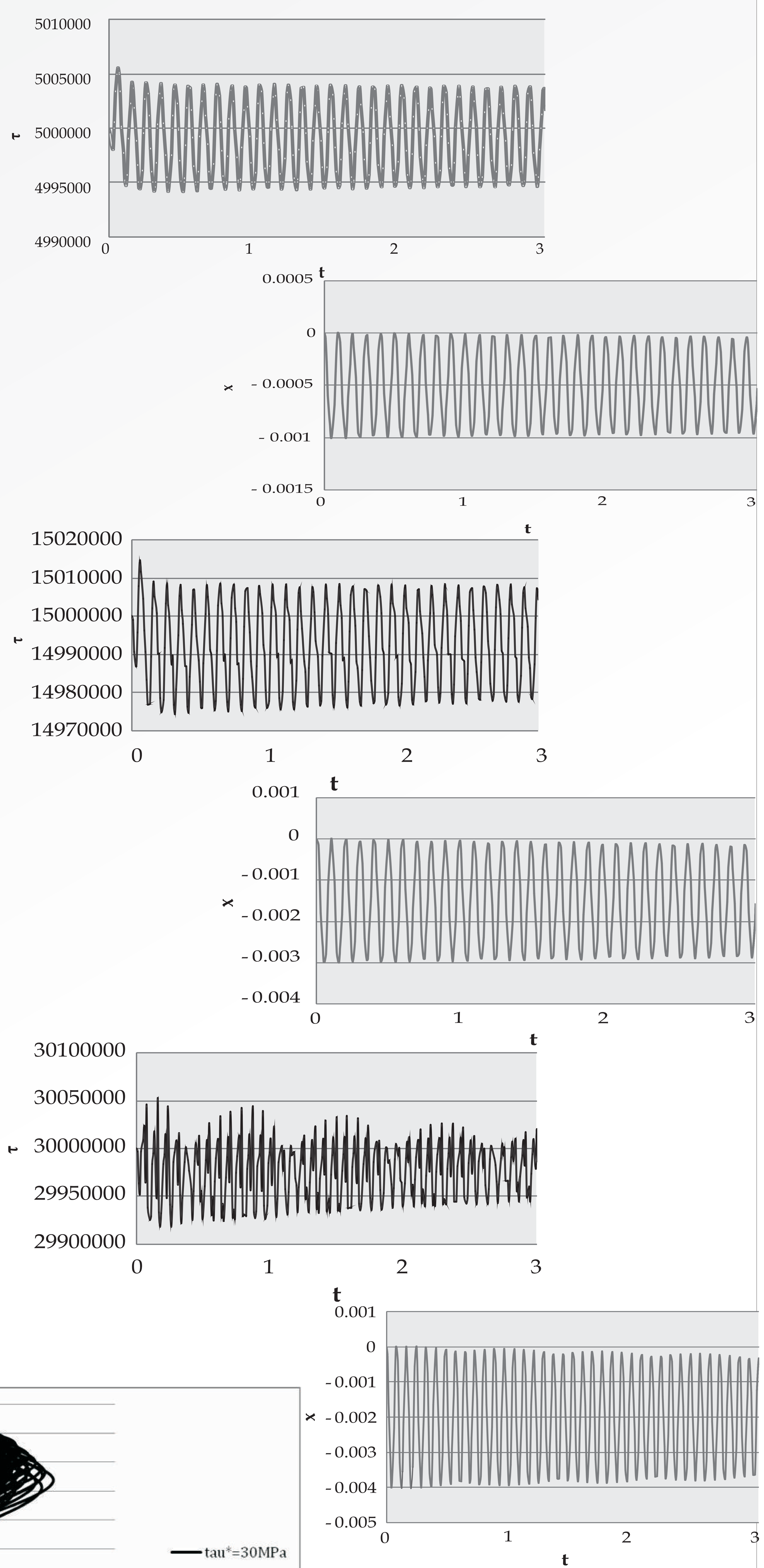

Fig.8. Dependencies of shear stresses τ on time t and displacement x on time t for several values of critical shear stresses (from up to down): τ*=5MPa; τ*=15MPa; τ*=45MPa.